PAPER REF: 2680

EXPERIMENTAL ASSESMENT OF INFRARED WELDED BONDS USING LAPSHEAR, DOUBLE CANTILEVER BEAM AND END NOTCH FLEXURE TESTS FOR A CARBON FABRIC REINFORCED THERMOPLASTIC

Klaas Allaer(*), Ives De Baere, Stefan Jacques, Wim Van Paepegem, Joris Degrieck
Department of Materials Science and Engineering, Faculty of Engineering and Architecture, Ghent University.
Technologiepark-Zwijnaarde 903, B-9052 Zwijnaarde, Belgium.
(*)*Email:* klaas.allaer @UGent.be

ABSTRACT

High performance composites, such as carbon-fibre reinforced plastics (CFRP), are increasingly being used in high engineering industries. Their wide acceptance introduces an issue regarding the bonding of these materials and their mechanical behaviour. As this reinforced thermoplastic is not easily bonded with adhesives due to the chemical inertness, the fusion bonding process could be used to make a structural bond. In this paper, the interlaminar fracture behaviour of infrared welded bonds was investigated based on experimental analysis. The material used, is a 5-harness satin-weave (5HS) carbon fabric-reinforced polyphenylene sulphide (PPS). Laminates were welded using infrared light and a delamination was introduced by a Kapton film. Welding parameters were first optimized using lapshear tests, then mode I and mode II tests were conducted to determine the fracture toughness behaviour of the welded bonds. Tests under mode I loading were carried out using double cantilever beam (DCB) specimens whereas for mode II loading, three-point end notched flexure (ENF) specimens were considered. Crack growth under mode I and mode II loading conditions was observed to be unstable resulting in a sawtooth like load-displacement response, but nevertheless, values for the fracture toughness were derived.

Keywords: Infrared welding, interlaminar fracture toughness, DCB, ENF

INTRODUCTION

The use of fibre reinforced thermoplastics for structural applications is continuously increasing and, therefore, load bearing joints cannot be avoided. As most well-established joining techniques for metallic structures are not directly applicable to composites and as thermoplastics are difficult to bond adhesively because of their chemical inertness, another solution is found, namely fusion bonding [Yousefpour (2004)]. For this research, specimens were bonded by use of the infrared welding technique. Welding parameters such as heating time, contact pressure and consolidation time have been optimized using lapshear experiments [De Baere, Allaer (2012)]. The background of this research was the investigation of the mechanical behaviour of composite fusion bonded joints and the present study is aimed at providing some additional experimental information of the interlaminar fracture toughness of the joints. The emphasis of this study lies on determining the fracture toughness and crack growth behaviour of infrared welded joint laminates. To predict failure behaviour in fibre

reinforced materials under different loading conditions, the resistance to delamination in terms of interlaminar fracture toughness has to be assessed. Already numerous methods have been proposed by researchers to determine the resistance to delamination for composite materials. [Sela (1989), Brunner (2008)]. These methods have been used on investigating the fracture toughness behaviour of materials, composite laminates with internal inserts and adhesively bonded joints, the approach has not yet been applied to infrared welded bonds. The double cantilever beam (DCB) test is the most widely used method for measuring mode I (opening) energy release rates. The end notched flexure (ENF) has emerged as one of the most convenient mode II (shear) type cracking test and therefore, will also be considered here. Linear elastic fracture mechanics is used for determining the interlaminar damage in a carbon fabric reinforced thermoplastic composite.

MATERIALS AND METHODS

The material under study is a carbon fabric reinforced polyphenylene sulphide (PPS) composite, called CETEX®, which was supplied by the company Ten Cate. The fibre type used is the carbon fibre T300J 3K and the weave pattern is a 5-harness satin weave, one stacking sequence was used for this study, namely $[(0^o, 90^o)]_{4s}$ where $(0^o, 90^o)$ represents one layer of fabric. The plates were produced by hot pressing at a temperature of 310 °C and a pressure of 10 bar. The in-plane elastic properties and the tensile strength properties of the CETEX® composite are listed in Table 1.

Table 1: Elastic and strength properties of the CETEX® material

E_{11} [GPa]	E_{22} [GPa]	ν_{12} [-]	G_{12} [GPa]	X_T [MPa]	ε_{11}^{ult} [-]	Y_T [MPa]	ε_{22}^{ult} [-]	S_T [MPa]
56.0	57.0	0.033	4.175	736	0.011	754.0	0.013	110.0

The test specimens for both loading conditions were joined together by use of a fusion bonding technique. For this research, the necessary heat is generated by using infrared light (Fig. 1).

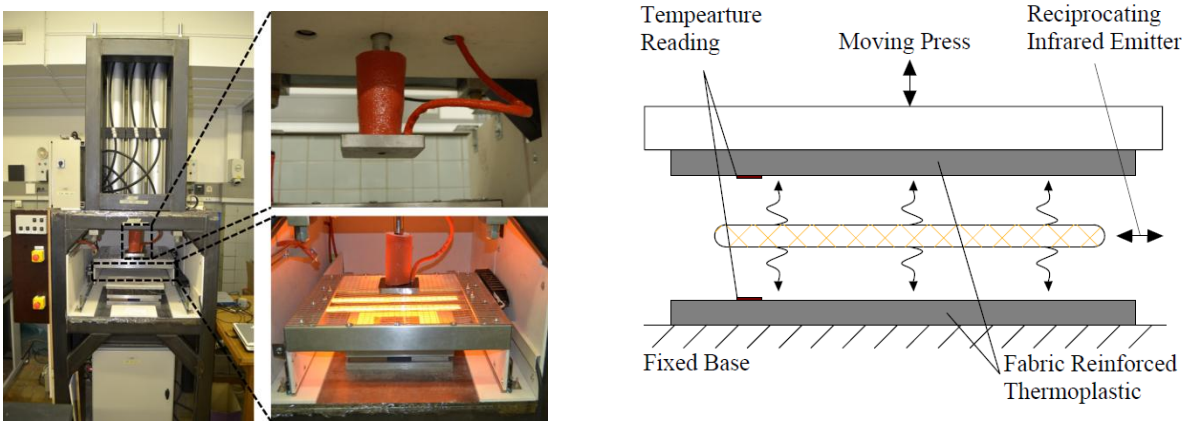

(a) Infrared welding machine (b) Infrared welding cycle

Fig. 1. Illustration of the used infrared welding procedure.

When the PPS has molten, both specimens are pushed together with a certain pressure and the liquid PPS consolidates. With the standard plates there is insufficient PPS to form a decent bond and extra layers of PPS are consolidated on the specimens in a separate phase, prior to welding. For the welding procedure the amount of PPS, the heating time, consolidation

pressure and consolidation time were optimized by evaluating lapshear test results of the welded bonds [De Baere, Allaer (2012)]. Fig. 2 illustrates some of the results from the optimization process, for every cycle 3 specimens were tested.

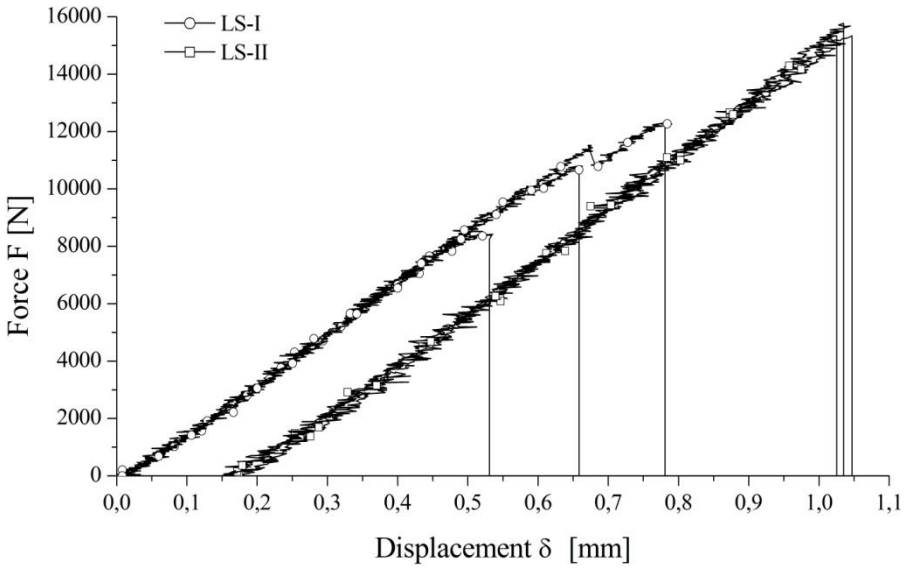

Fig. 2. Relation between load and displacement for lapshear tests.

As the welding procedure was optimized it was found that the welding process where thermoplastic matrix material is welded on the adherends prior to the actual welding, gives higher lapshear strength and very reproducible results (Fig. 2). In Table 2 the process parameters for the welding process are summarized. The process consist of two phases: 1) melting and subsequently pressing additional PPS material onto both adherend surfaces, and 2) welding both adherends together.

Table 2: Welding parameters for the welding procedure.

Welding cycle	Pressure [MPa]	t_{melt} [s]	$t_{consolidate}$ [s]
Phase-1	0.7	125	235
Phase-2	0.7	115	280

As delamination initiator a non-adhesive Kapton film was inserted in the mid-plane of the laminate during welding. The test specimens for mode I and mode II experiments were sawn with a water cooled diamond saw. The dimensions and geometry of the double cantilever beam and end notched flexure specimens are shown in Fig. 3. To initiate the crack growth all specimens were pre-cracked.

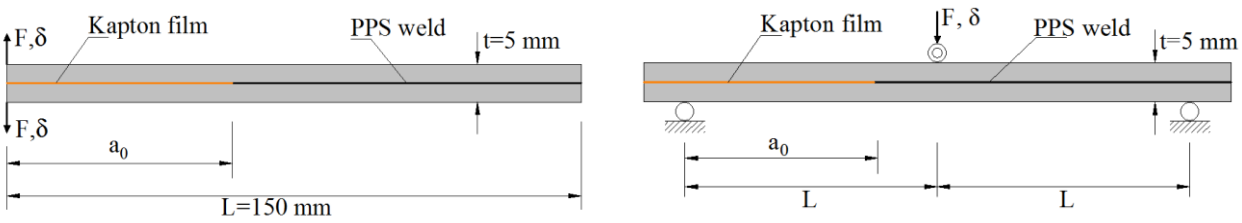

(a) DCB (double cantilever beam)

(b) ENF (end notched flexure)

Fig. 3 Dimensions and geometry of mode I (DCB) and mode II (ENF) specimen

All tensile tests were performed on an electromechanical INSTRON 5800R tensile testing machine with a FastTrack 8800 digital controller and a load cell of ±10kN. The quasi-static tests were displacement-controlled with a rate of 0.5 mm/min. For the registration of the tensile data a combination of a National Instruments USB 6251 data acquisition card and a SCB-68 pin shielded connector were used. The load F and displacement δ, given by the FastTrack controller, were sampled on the same time basis.

EXPERIMENTAL RESULTS AND DISCUSSIONS

Double Cantilever Beam test (Mode I)

The DCB specimens are tested in a tensile testing machine where a tensile load is applied at adhesively bonded hinges. There are several ways in which initiation and propagation values of G_{IC} can be derived from the recorded load-displacement data [ASTM (1994)]. Initiation of delamination is determined by deviation from linearity. Here G_{IC} can be calculated using the load and displacement at the point of non-linearity of the load-displacement curve. From Fig. 4 it can be seen that the crack growth is unstable, several periods of no delamination growth are followed by a rapid delamination, yielding sharp drops in the load-displacement curve with virtually infinite slope.

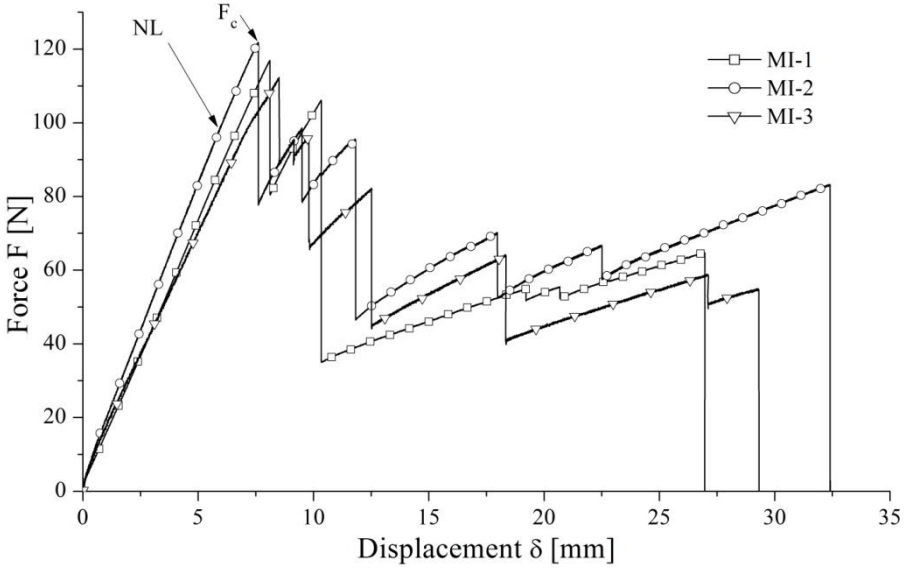

Fig. 4. Relation between load and displacement for mode I fracture toughness test

The relation between the force F and corresponding displacement δ is given by [Turon (2010)]:

$$F = \sqrt{\frac{G_{IC}\, b^2 h^3 E_{11}}{12a^3}} \qquad \text{and} \qquad \delta = F\frac{8a^3}{bh^3 E_{11}} \tag{1}$$

where G_{IC} is the critical energy release rate, b the specimen width, h half the specimen thickness, E_{11} Young's modulus in the warp direction and a the delamination length. Eliminating the delamination length a in Equations (1) yields an expression to determine the critical energy release rate for mode I loading conditions:

$$G_{IC} = 3\left(\frac{\sqrt{\delta}F_c}{b(h^3 E_{11})^{1/4}}\right)^{4/3} \tag{2}$$

where F_c gives the critical force at crack propagation. Since it is impossible to record delamination length readings during the unstable crack growth propagation of the delamination, fracture toughness is calculated from the maximum force point of the load-displacement curve. During the DCB experiments all specimens exhibited similar saw-toothed load-displacement behaviour due to unstable crack growth making it difficult to accurately determine critical energy release rates from the curves. By taking the first peak force F_c of the curve and fitting a LEFM-based model on this value, values for G_{IC} propagation of the crack can be derived. The curve exhibits a non-linear response after a linear response region until a sudden load drop. The crack initiation point is given at the point of non-linearity and yields the initiation critical energy release rate $G_{IC,ini}$. When no non-linear section is noticeable before the first force drop, another method could be used to obtain the initiation energy release rate [De Baere, Jacques (2012)]. Calculation of the propagation energy release rate is done fitting Equation (2) on the experimental data using the point of maximum force as the critical force F_c. Table 3 summarizes the results of mode I initiation and propagation energy release rates.

Table 3: Interlaminar fracture properties under mode I loading

Specimen	$G_{IC,ini}$ [N/m]	$G_{IC,prop}$ [N/m]
MI-1	672	1013
MI-2	663	1021
MI-3	680	1002

From the mode I experimental values it can be seen that in comparison with hot pressed bonding welded joints have a bigger resistance for crack propagation, on the other hand the initiation fracture toughness is lower [De Baere, Jacques (2012)]. Smaller and more frequent force drops were observed during the mode I experiment with the hot pressed specimens.

End Notched Flexure test (Mode II)

An ENF test involves performing a three-point bending test on a specimen with initial delamination at one end. While applying a load onto the specimen the initial delamination will grow towards the central loading roller under sliding shear conditions.

Obtaining the critical energy release rate for mode II requires a reduction of the load-displacement data from the experimental tests. Similarly to the DCB tests, crack length growth could not be recorded due to unstable crack propagation. Classical data reduction schemes [Brunner (2000), Blackman (2006), Brunner (2008)] do not take into account the fracture process zone effects such as material property degradation ahead of the crack tip, micro-cracking and inelastic processes which have the tendency to close the crack under the shear loading conditions. Here mode II energy release rate is calculated using the Compliance-Based Beam Method [Srinivasan (2009), de Moura (2009)], which account for the fracture process zone effects.

Implementation of the Compliance-Based Beam Method requires a geometrical boundary condition, $a_0/L \geq 0.7$, to ensure stable crack growth. The method depends only on the equivalent crack length a_{eq} and the specimen compliance $C = \delta/F$. The compliance during crack growth is given as:

$$C = \frac{3a_{eq}^3 + 2L^3}{8E_f bh^3} + \frac{3L}{10G_{13}bh} \tag{4}$$

where $a_{eq} = a + \Delta a_{FPZ}$, the equivalent delamination length with a the crack length and Δa_{FPZ} the correction for the fracture process zone effect, E_f the flexural stiffness, L half the span length, b the width of the specimen and h half the specimen height. The specimen compliance requires the input of G_{13} of the material which is determined by meso-scale modeling [Daggumati (2010)]. Flexural stiffness E_f is a function of the initial delamination length a_0 and the compliance C_0 of the linear part on the load-displacement curve (Fig. 5). From equation (4) follows that:

$$E_f = \frac{3a_0^3 + 2L^3}{8E_f b h^3 C_{0,corr}} \tag{5}$$

The equivalent delamination length a_{eq} during crack propagation can be derived from Equation (4) and (5)

$$a_{eq} = \left[\frac{C_{corr}}{C_{0,corr}} a_0^3 + \frac{2}{3}\left(\frac{C_{corr}}{C_{0,corr}} - 1\right) L^3\right]^{1/3} \tag{6}$$

$$\text{with} \quad \begin{cases} C_{corr} = C - \dfrac{3L}{10 G_{13} b h} \\ C_{0,corr} = C_0 - \dfrac{3L}{10 G_{13} b h} \end{cases}$$

This data reduction scheme excludes the tracking of the crack length a during loading of the specimen. Mode II critical energy release rate G_{IIC} is determined as follows:

$$G_{IIC} = \frac{9F^2 a_{eq}^2}{16 b^2 E_f h^3} \tag{7}$$

When stable crack growth is observed during experimental testing the load-displacement curve has a continuous shape (Fig. 5 (b)). The load-displacement response from the ENF test is shown in Fig. 5 (a). The initial compliance curve (C_0) states the position of the non-linear point NL, propagation of the crack starts at the first point of maximum force F_c. In the load-displacement curves no zone of decreasing force with increasing crack growth and thus increasing equivalent crack length a_{eq} is observed. Unstable crack growth is noticeable when the first peak force F_c is reached.

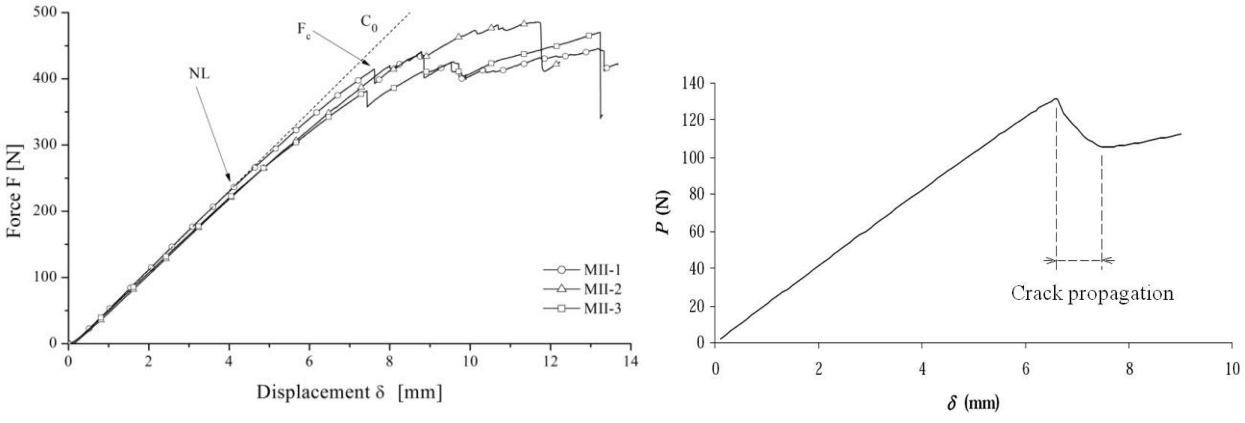

(a) Unstable crack growth (b) Stable crack growth [Srinivasan (2009)]

Fig. 5. Relation between load and displacement for mode II fracture toughness test

The initiation fracture energy $G_{IIC,ini}$ corresponding to the initiation of growth, was taken at the onset of non-linearity (NL) of the load-displacement curve. Using Equation (7) the resistance curve or R curve can be derived. Fig. 6 illustrates the shape of the resistance curve which has no unique plateau due to the unstable delamination growth, other results gave similar R-curves but for simplicity only one is illustrated.

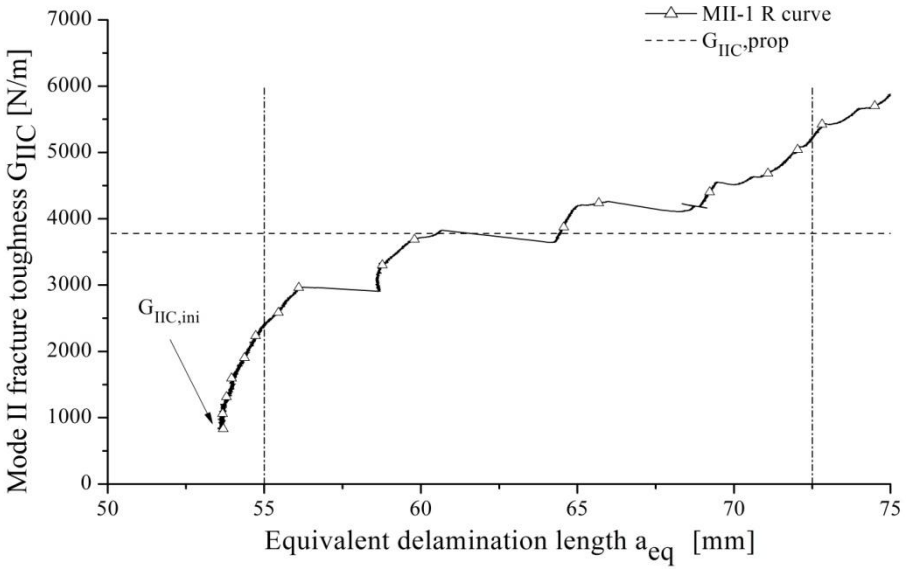

Fig. 6. Relation between mode II fracture toughness and equivalent delamination length.

Since one unique propagation value could not be extracted from the R-curve an averaged propagating energy release rate was taken from the several plateaus in the R curve. Table 4 summarizes the results for mode II initiation and propagation energy release rates, more experiments were conducted which verify the measurement reproducibility.

Table 4: Interlaminar fracture properties under mode II loading

Specimen	$G_{IC,ini}$ [N/m]	$G_{IC,prop}$ [N/m]
MII-1	871	3855
MII-2	859	3778
MII-3	863	3705

In can be seen from the experimental values that reproducible results were obtained during the tests. For the mode II initiation fracture toughness an averaged value $G_{IIC,ini}$ of 865 N/m was calculated, for the propagating fracture toughness a value of 3780 N/m was derived. Comparing to hot pressed bonds crack resistance against propagation is higher when using welded joints [De Baere, Jacques (2012)].

CONCLUSIONS

In this study, interlaminar fracture toughness tests were conducted in mode I and mode II for infrared fusion bonded 5HS fibre reinforced thermoplastic joints. Interlaminar fracture toughness was determined experimentally using double cantilever beam and end notched flexure tests. No stable crack propagation could be observed and saw-tooth load-displacement responses were recorded. Both initiation and propagation critical energy release rates for the two loading conditions were extracted from the experiments. The average initial value $G_{IC,ini}$

for fracture propagation in mode I was found to be 672 N/m, whereas the average propagation value $G_{IC,prop}$ of the mode I interlaminar fracture toughness is 1012 N/m. The Compliance-Based Beam Method was used as a data reduction scheme for extracting both critical energy release rates in mode II loading conditions. A value of 865 N/m was found for the initiation of fracture $G_{IIC,ini}$ and 3780 N/m for propagation fracture toughness $G_{IIC,prop}$. Comparing the mode I and mode II fracture toughness behaviour of the infrared welded and hot pressed joined laminates, it was observed that the force drops during propagation of the delamination are larger and less frequent for welded bonds. For mode I and mode II crack propagation in welded bonds was found to be unstable whereas in hot pressed joints unstable crack growth was only noticed in mode I.

ACKNOWLEDGMENTS

The authors are highly indebted to the Fund of Scientific Research – Flanders (F.W.O.) for sponsoring this research and to Ten Cate Advanced Composites for supplying the material.

REFERENCES

ASTM. Standard test method for mode I interlaminar fracture toughness of unidirectional fibre-reinforced polymer–matrix composites. D5528, ASTM 1994.

Blackman BRK, Brunner AJ, Williams JG. Mode II fracture testing of composites: a new look at an old problem. Engineering Fracture Mechanics, 2006, 73, p. 2443-2455.

Brunner AJ, Blackman BRK, Davies P. A status report on delamination resistance testing of polymer-matrix composites. Engineering Fracture Mechanics, 2008, 75, p. 2779-2794.

Brunner AJ. Experimental aspects of Mode I and Mode II fracture toughness testing of fibre-reinforced polymer-matrix composites. Computer Methods in Applied Mechanics and Engineering, 2000, 185, p. 161-172.

Daggumati S, Van Paepegem W, Degrieck J, Xu J, Lomov SV and Verpoest I. Local damage in a 5 – harness satin weave composite under static tension: part II - meso – FE modeling. Composites Science and Technology 70, 13, 2010, p. 1934-1941.

De Baere I, Allaer K, Jacques S, Van Paepegem W, Degrieck J. Study of the interlaminar behaviour of infrared welded joints of carbon fabric reinforced polyphenylene sulphide, Submitted to Polymer Composites, 2012.

De Baere I, Jacques S, Van Paepegem W, Degrieck J. Study of the Mode I and Mode II interlaminar behaviour of a carbon fabric reinforced thermoplastic, Polymer Testing, 31, 2, 2012, p. 322-332.

De Moura MFSF, Campilho RDSG. Gonçalves JPM. Pure mode II fracture characterization of composite bonded joints. International Journal of Solids and Structures, 2009, 46, p. 1589-1595.

Sela N, and Ishai O. Interlaminar fracture-toughness and toughening of laminated composite materials - A review. Composites 20, 5, 1989, p. 423-435.

Srinivasan Sridharan. Delamination behaviour of composites. Cambridge: Woodhead Publishing Limited, Boca Raton: CRC Press LLC, 2008.

Turon A, Camanho PP, Costa J And Renart J. Accurate simulation of delamination growth under mixed-mode loading using cohesive elements: definition of interlaminar strengths and elastic stiffness. Composite Structures 92, 8, 2010, , p. 1857-1864.

Yousefpour A, Hojjati M, Immarigeon JP. Fusion bonding/welding of thermoplastic composites. Journal of Thermoplastic Composite Materials, 2004, 4, p. 303-341.